# Competing spring constant versus double resonance effects on the properties of dispersive modes in isolated single-wall carbon nanotubes

A. G. Souza Filho,[1,2,*] A. Jorio,[1,3] Ge. G. Samsonidze,[4] G. Dresselhaus,[5] M. A. Pimenta,[3] M. S. Dresselhaus[1,4]
Anna K. Swan,[6] M. S. Ünlü,[6] B. B. Goldberg[6,7] and R. Saito[8]
[1]*Department of Physics, Massachusetts Institute of Technology, Cambridge, Massachusetts 02139-4307*
[2]*Departamento de Física, Universidade Federal do Ceará, Fortaleza-CE, 60455-760, Brazil*
[3]*Departamento de Física, Universidade Federal de Minas Gerais, Belo Horizonte–MG, 30123-970 Brazil*
[4]*Department of Electrical Engineering and Computer Science, Massachusetts Institute of Technology, Cambridge, Massachusetts 02139-4307*
[5]*Francis Bitter Magnet Laboratory, Massachusetts Institute of Technology, Cambridge, Massachusetts 02139-4307*
[6]*Electrical and Computer Engineering Department, Boston University, Boston, Massachusetts 02215*
[7]*Department of Physics, Boston University, Boston, Massachusetts 02215*
[8]*Department of Electronic-Engineering, University of Electro-Communications and CREST-JST, Tokyo, 182-8585, Japan*
(Received 2 July 2002; revised manuscript received 16 September 2002; published 31 January 2003)

We report a study of the disorder-induced *D* band in the resonance Raman spectra of isolated single-wall carbon nanotubes (SWNTs). We show that the *D*-band frequency $\omega_D$ depends directly on the nanotube diameter $d_t$ and also on the magnitude of the wave vector for the quantized states $k_{ii}$, where the van Hove singularities in the density of states occur. These two effects are manifested in the *D*-band frequency through the $\omega_D = \omega_D^0 + C/d_t$ functional form, but with $C$ negative (positive) for the spring-constant- (double-resonance-) dependent processes, thereby indicating that the spring constant softens and the double resonance stiffens the *D*-band frequencies. In the case of the spring constant effect, $\omega_D^0$ is the frequency observed in two-dimensional graphite. The outcome of the softening versus stiffening competition depends on the nanotube diameter range. When plotted over a wide $d_t$ range, the diameter dependence of $\omega_D$ ($C<0$) arises from the softening of the spring constants due to the nanotube curvature, but within a single interband transition $E_{ii}$, whereby the $d_t$ variation is small, the *D*-band stiffening ($C>0$) due to the double-resonance condition becomes the dominant effect.

DOI: 10.1103/PhysRevB.67.035427 PACS number(s): 78.30.Na

## I. INTRODUCTION

Single-walled carbon nanotubes (SWNTs) have attracted much attention owing to their very special physical properties, which are related to their one-dimensional (1D) character, making them ideal materials for studying physical phenomena in one-dimensional solids.[1,2] Among the various experimental techniques that have been employed to study SWNTs in bundles or ropes and in composites, Raman spectroscopy has become established as a dominant characterization technique for determining the SWNT diameter $d_t$ (since the radial breathing mode frequency exhibits a nanotube diameter dependence $\omega_{\mathrm{RBM}} \propto 1/d_t$) for the small subset of SWNTs that are in resonance with $E_{\mathrm{laser}}$, based on the so-called diameter-selective resonance Raman scattering effect.[3,4]

A new research field in SWNTs was opened up by observing Raman spectra from just one isolated single-wall carbon nanotube.[5] The observation of Raman spectra from just one nanotube is possible because of the very large density of electronic states close to the van Hove singularities in the joint density of electronic states (JDOS) (Ref. 6) of this 1D structure. By combining the resonant process with several new physical phenomena related to the dependence of the SWNT electronic structure on the nanotube diameter and chirality $\theta$, the phonon spectra have been successfully used for the structural characterization of isolated SWNTs, which means to experimentally determine their $(n,m)$ structural indices.[5,7]

Associated with a double-resonance process,[8–10] the dispersive disorder-induced *D* mode in SWNTs is also very important for characterizing SWNTs, because its properties, including its frequency, intensity, and linewidth, carry information about SWNT electronic properties, their compressive or tensile strain, and the degree of structural disorder of the SWNT. Such information turns out to be decisive for achieving high mechanical performance, thereby allowing use of this mode for characterizing and also monitoring the purification process of SWNTs. The observation of the second-order $G'$ band (a *D*-band overtone) is not defect dependent, but its frequency is strongly dependent on compressive and tensile strain, with observed pressure coefficients for the $G'$-band frequency in SWNT bundles of $\sim 23\ \mathrm{cm}^{-1}/\mathrm{GPa}$ (under compression) and $-13\ \mathrm{cm}^{-1}/\mathrm{GPa}$ (under tension),[11–13] and these properties can be used to characterize nanotubes, making Raman spectroscopy a sensitive technique for verifying either compressive or tensile strain effects in SWNTs. Gaining an understanding of the mechanisms responsible for this behavior for both semiconducting and metallic tubes is one of the goals of the present paper.

Previous studies of isolated SWNTs have shown that the *D*-band frequency $\omega_D$ depends on the nanotube diameter, with $\omega_D$ increasing as the nanotube diameter increases.[14] The

 

use of a high-nanotube-density sample ($\sim$10 SWNTs/$\mu$m$^2$ or per laser spot) did not allow us (Ref. 14) to perform a quantitative detailed study of the diameter dependence of the *D*-band features. A more detailed study later revealed the role of the quantized wave vectors $k_{ii}$ (where $k_{ii} \propto 1/d_t$ and $k_{ii}$ is the wave vector corresponding to the singularity in the joint density of electronic states) in determining the *D*-band frequencies[15] owing to the double-resonance phenomenon that strongly couples phonons and electrons.[8–10] Two effects sensitively modify $\omega_D$, the first coming from the softening of the spring constants due to the nanotube curvature and the second coming from the double-resonance effect. Both of these phenomena affect the functional form of the *D*-band frequency $\omega_D = \omega_D^0 + C/d_t$, where $C$ is negative (positive) for the spring constant (double resonance) $d_t$ dependence. In the case of the spring constant effect $\omega_D^0$ is the frequency observed in 2D graphite. The goal of this paper is to clarify the roles of these two competing (softening versus stiffening) behaviors in controlling the magnitude of $\omega_D$. A comparison with $\omega_D$ for SWNT bundles is also obtained by appropriately averaging the $\omega_D$ data for the isolated SWNTs.

## II. EXPERIMENT

The details of the sample preparation are reported elsewhere.[16] Raman spectra from each isolated SWNT were obtained by scanning the sample in steps of 0.5 $\mu$m under a controlled microscope stage. The spectral excitation was provided by an Ar ion laser, using the 514.5 nm laser line (2.41 eV) and with a power density of $\sim$1 MW/cm$^2$ on the sample surface. We also used a Ti:sapphire laser (1.58 eV) to excite the Raman spectra. The scattered light was analyzed with a Renishaw spectrometer 1000B and a Kaiser optical spectrograph Hololab 5000R, equipped with a cooled charge-coupled device (CCD) detectors.

## III. RESULTS AND DISCUSSION

### A. *D*-band diameter dependence

Figure 1(a) shows data [for both semiconducting (*S*) and metallic (*M*) tubes probed with $E_{\text{laser}} = 2.41$ eV] for the *D*-band frequency $\omega_D$ for isolated SWNTs plotted versus $1/d_t$ for different interband electronic transitions $E_{ii}$, coinciding with singularities in the JDOS. Although these data are all taken with the same laser excitation energy, the data points do not show a definitive pattern. We can, however, see that $\omega_D$ for isolated SWNTs has lower values than $\omega_D$ for 2D graphite (1355 cm$^{-1}$ taken from Ref. 17, as shown by the solid diamond point in Fig. 1). The data points in Fig. 1(a) seem to extrapolate roughly to the 2D graphite[17] value when $d_t \to \infty$, i.e., $(1/d_t) \to 0$, consistent with a previous investigation[14] where this behavior was reported qualitatively. However, the experimental measurements for the dependence of $\omega_D$ on the diameter $d_t$ (see Fig. 1) do not deliver a clear message when taken by themselves at the single-nanotube level, but as we will further see, these data are very useful for understanding the corresponding effect in SWNT bundles. As we show below, the spread in the data points in

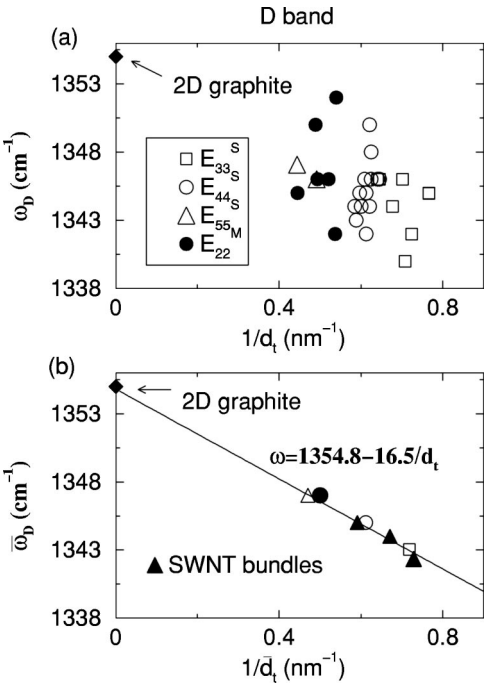


FIG. 1. (a) *D*-band frequencies as a function of reciprocal diameter for individual SWNTs using $E_{\text{laser}} = 2.41$ eV laser excitation. The data are classified in terms of the $E_{ii}$ interband transition with which the resonance occurs, including both metallic (*M*) and semiconducting (*S*) SWNTs. (b) Plot of $[\overline{\omega_D(E_{ii})}]$, denoting the observed *D*-band frequencies averaged over all tubes resonant with a given interband transition $E_{ii}$ vs $1/\overline{d_t}$, the corresponding average of the reciprocal diameter of the tubes. Data are shown for $E_{\text{laser}}$ in resonance with the $E_{55}^S$, $E_{44}^S$, $E_{33}^S$, and $E_{22}^M$ interband transitions in the JDOS. The line is a fit to the data, showing that the *D*-band frequencies extrapolate (on average) to the graphene (2D graphite) value when $1/\overline{d_t} \to 0$. The solid triangles in (b) denote the *D*-band frequencies for three different SWNT bundles with different average diameters (Refs. 19–21).

Fig. 1(a) is associated with the chirality dependence[15] of the $k_{ii}$ states as a consequence of the trigonal warping effect[18] and the double-resonance process.[8,9]

What we mean by the chirality dependence for SWNTs is that different nanotubes with different $d_t$ and $\theta$ values will be resonant at the same $E_{\text{laser}}$ value, thus giving rise to a range of $\omega_D$ values, whereas for $sp^2$ carbons and graphite, there is a single $\omega_D$ for a given $E_{\text{laser}}$. The same situation applies to the $G'$ band. In Ref. 15 we reported that $\omega_D$ has a dependence on chiral angle $\theta$ for nanotubes with a similar diameter, whereas $\omega_{\text{RBM}}$ and $\omega_G$ do not show any significant dependence on $\theta$.[7] The detailed dependence of $\omega_D$ on chirality for the $E_{33}^S$ and $E_{44}^S$ transitions and their relation with the quantized wave vectors $k_{ii}$ are discussed in our previous paper.[15]

In order to compare the results at the single-nanotube level with those for SWNT bundles and to gain an understanding of the mechanisms behind the $d_t$ dependence of the *D*-band frequency, we average over the chirality-dependent $\omega_D$ data for the isolated SWNTs shown in Fig. 1(a) for a given interband transition $E_{ii}$, over which the $d_t$ values

show only a small variation. We denote the resulting averages of the diameter and *D*-band frequencies by $\overline{d_t}(E_{ii})$ and $\overline{\omega_D}(E_{ii})$, respectively, and we plot these pairs of numbers in Fig. 1(b) for $i=3,4,5$ for semiconducting and for $i=2$ for metallic SWNTs, using the same symbols as in Fig. 1(a). The metallic tubes are distinguished from semiconducting tubes by the Breit-Wigner-Fano (BWF) line shape for the lower-frequency component of the *G*-band spectra (denoted by $G^-$).[22] To distinguish between metallic and semiconducting SWNTs for larger-diameter tubes for which the BWF line shape is often not clearly evident for metallic tubes, we also use the magnitude of the splitting $\Delta\omega_G=\omega_{G^+}-\omega_{G^-}$, which is known to be quite different for metallic and semiconducting tubes,[22] and $\Delta\omega_G$ for metallic tubes[22] is given by the relation $\Delta\omega_G=C/d_t^2$, where $C$ is 79.5 $\mathrm{cm}^{-1}$ $\mathrm{nm}^2$.

The results of this analysis in Fig. 1 give a simple linear dependence of $\overline{\omega_D}$ on $1/\overline{d_t}$, i.e.,

$$\overline{\omega_D}=1354.8-16.5/\overline{d_t}, \tag{1}$$

where $1/\overline{d_t}$ is the average of $1/d_t$, as shown in Fig. 1(b). We also obtain very good agreement in Fig. 1(b) between the $\overline{\omega_D}$ results for isolated tubes and the corresponding $\overline{\omega_D}$ results for SWNT bundles measured with the same $E_{\mathrm{laser}}$. The solid triangles in Fig. 1(b) denote the average $\overline{\omega_D}$ for SWNT bundles with different average SWNT reciprocal diameters $1/\overline{d_t}$, as given in Refs. 19–21. The results of Fig. 1(b) show that $\overline{\omega_D}(E_{ii})$ for isolated SWNTs and $\overline{\omega_D}$ for SWNT bundles both increase when $d_t$ increases, and both data sets yield the same functional form. The linear downshift of $\overline{\omega_D}$ as a function of $1/\overline{d_t}$, shown in Fig. 1(b), is attributed to the softening of the spring constants for the vibrations associated with the *D* band due to the nanotube curvature. This assertion is based on calculations of the eigenvectors for the *D* band[23] which show that the atomic displacements have some components along the nanotube circumference, which soften the modes due to some contributions from out-of-plane force constants. Contributions from out-of-plane force constants also are responsible for the $d_t$-dependent lowering of $\omega_{G^-}$, the lower-frequency circumferential component of the *G* band.[24,25]

However, when we investigate the behavior of $\omega_D$ vs $d_t$ at the single-nanotube level, within one interband transition—$E_{44}^S$, for example—the *D*-band frequency $\omega_D$ has a tendency to *increase* when the diameter decreases,[15] because $E_{ii}$ is proportional to $k_{ii}$, which in turn is proportional to $1/d_t$, except for perturbations due to the trigonal warping effect, which complicate this simple dependence and give rise to a spread in the data points [see Fig. 1(a)].[1] The net result of the effect due to the formation of $E_{ii}$ subbands in this 1D system is to introduce an opposite dependence of $\omega_D$ on $d_t$ when compared to the averaged result shown in Fig. 1(b). Since for a given interband transition $E_{ii}$ the relevant tube diameter range is not so large, the frequency of the *D* band, $\omega_D$, is mainly determined by the magnitude of the $k_{ii}$ states,[15] and this effect is dominant over the curvature effect throughout the small diameter range where contributions from resonance within a single $E_{ii}$ subband dominate. When we jump from one van Hove singularity $E_{ii}$ to another singularity $E_{i'i'}$, the spring constant mechanism becomes dominant in the determination of $\omega_D$.

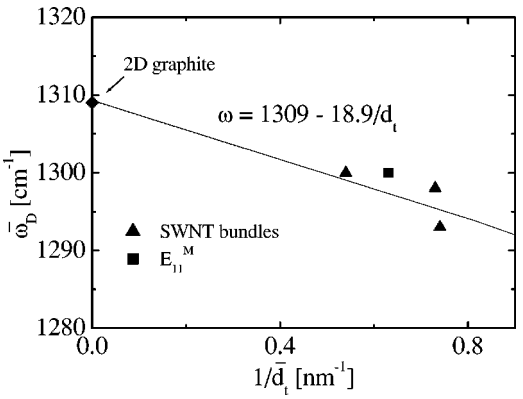


FIG. 2. Plot of the average *D*-band frequencies as a function of reciprocal average diameter for Raman spectra taken with $E_{\mathrm{laser}}=1.58$ eV. The solid square data point is obtained by averaging over $\omega_D$ and $1/d_t$ for 14 individual metallic SWNTs in resonance with the $E_{11}^M$ interband transition. The solid triangles denote *D*-band frequencies for three different SWNT bundles with different average diameters, but in the range where resonance with metallic tubes is highly favorable (Ref. 19,20). The line is a fit to the data, showing that the *D*-band frequencies extrapolate (on average) to the graphene (2D graphite) value when $1/\overline{d_t}\rightarrow 0$. $\omega_D$ for 2D graphite was taken by extrapolating the data from Ref. 28 for $E_{\mathrm{laser}}=1.58$ eV.

The results shown in Fig. 1 also suggest that metallic and semiconducting tubes have the same $\omega_D$ diameter-dependent behavior. In order to delve deeper into this issue, we now analyze the corresponding results for metallic tubes for the SWNTs in resonance with $E_{11}^M$. The same analysis for metallic tubes is more difficult because the $E_{ii}^M$ electronic transitions are well separated in energy, and to measure both the $E_{11}^M$ and $E_{22}^M$ transitions with the same laser line, a very broad diameter distribution of isolated tubes is needed. Thus, the use of the laser line 1.58 eV on our isolated SWNT sample probes only the resonance with $E_{11}^M$, while the laser line 2.41 eV probes only SWNTs in resonance with $E_{22}^M$ as shown in Fig. 1.

Figure 2 shows the average $\overline{\omega_D}$ plotted versus the average $1/\overline{d_t}$ for the $E_{11}^M$ electronic transition for 14 different isolated SWNTs (solid square) and SWNT bundles (solid triangles) using $E_{\mathrm{laser}}=1.58$ eV. The values for $d_t$ were found by analyzing the radial breathing mode frequencies. Similar to the behavior shown in Fig. 1 for $E_{\mathrm{laser}}=2.41$ eV, a diameter dependence of $\overline{\omega_D}$ is observed for $E_{\mathrm{laser}}=1.58$ eV in Fig. 2 that is consistent with the results in Fig. 1 and with the values previously measured in SWNT bundles with different average diameters[19,26] (see triangles in Fig. 2). The different intercepts of $\omega_D$ in the limit $1/d_t\rightarrow 0$ in Figs. 1 and 2 reflect the double-resonance dispersion effect of $\partial\overline{\omega_D}/\partial E_{\mathrm{laser}}=50$–$53$ $\mathrm{cm}^{-1}/\mathrm{eV}$ for 2D graphite.[19,27,28] The slope in the dependence of $\overline{\omega_D}$ on $1/\overline{d_t}$ (18.9 $\mathrm{cm}^{-1}\mathrm{nm}$) for SWNTs in resonance with $E_{11}^M$ is, within the fitting error, the same as

that determined for SWNTs in resonance with $E_{22}^{M}$, $E_{33}^{S}$, $E_{44}^{S}$, and $E_{55}^{S}$ at $E_{\text{laser}}=2.41$ eV. This result suggests that the *D*-band diameter dependence for both semiconducting and metallic SWNTs is similar, showing that the effect of the softening of the spring constants on $\overline{\omega}_D$ seems to be the same, within our experimental error, for semiconducting and metallic tubes.[1] If we consider only the data for the average of the 14 isolated tubes (solid square in Fig. 2), the value for the average slope for the isolated tubes resonant with $E_{11}^{M}$ in Fig. 2 is even closer (15.0 $\text{cm}^{-1}$nm) to the value 16.5 $\text{cm}^{-1}$nm determined for the isolated tubes in Fig. 1. The spread in the data points for bundles might be due to several effects, such as different heating effects or different SWNT intertube interactions in the different bundle samples. These phenomena in SWNT bundles containing different numbers of SWNTs affect the measured *D*-band frequencies, and metallic tubes should be more susceptible to these effects than semiconducting tubes.

We have previously discussed the roles of the double-resonance effects versus the softening of the spring constants for explaining the experimental results presented above for the *D*-band frequencies for isolated SWNTs. Further evidence for corroborating the interplay between these two effects is also suggested by other experiments on SWNT bundles and on graphite.[12,13,29] The $G'$-band frequency under compressive strain shows a large variation (23 $\text{cm}^{-1}$/GPa) in comparison, for example, with 8.8 $\text{cm}^{-1}$/GPa for the tangential modes (*G*-band).[30] The large value of $\partial\omega_{G'}/\partial P$ can be attributed to the sum of two effects. First, the compressive strain increases the spring constant values, resulting in an upshift of the $G'$-band frequencies. Second, the compressive strain also upshifts the energy $E_{ii}$ of the quantized states, which turns out to increase the magnitude of the $k_{ii}$ wave vectors, thus contributing to an additional increase in the $G'$-band frequency.[31]

From the above discussion, we have determined the diameter dependence of $\omega_D$. We are now in a position to discuss and compare the general behavior of the Raman mode frequencies as a function of diameter for the most important features in the Raman spectra of SWNTs, including the radial breathing mode (RBM), the *G* band, the dispersive *D* and $G'$ bands (see Sec. III B for details), and some combination modes called the *M* band (a doublet feature that has been assigned as arising from a double-resonance process involving modes close to the $\Gamma$ point, the out-of-plane branch).[32] All mode frequencies observed in SWNT Raman spectra are, after performing the appropriate averages, related to the average diameter through the general relation

$$\overline{\omega}(d_t)=\omega_0+C/\overline{d_t^{\,n}}, \tag{2}$$

where *n* is an integer and $\omega_0$ is the frequency observed for 2D graphite, i.e., when $1/d_t\rightarrow 0$ for the double-resonance modes. It should be pointed out that for SWNT bundles, the general relation of Eq. (2) has also been used to describe $\omega_{\text{RBM}}$. In the case of the RBM, $\omega_0$ is not related to 2D graphite because the RBM is an intrinsic mode of SWNTs with no counterpart in graphite, but $\omega_0$ rather involves the intertube interaction within the SWNT bundle and from this intertube interaction $\omega_0$ has been evaluated as 14 $\text{cm}^{-1}$.[31]

TABLE I. Diameter dependence of the most intense features observed in the Raman spectra of isolated SWNTs. Here $\omega_0$ denotes the mode frequency associated with 2D graphite, whose value depends on the laser excitation energy. Frequencies are in units of $\text{cm}^{-1}$, and $d_t$ is in units of nm. The coefficients for the *D*, *M*, and $G'$ bands and for the RBM were obtained by using data measured with $E_{\text{laser}}=2.41$ eV (1.58 eV).

| $\overline{\omega}=\omega_0+C/\overline{d_t^{\,n}}$ | | | |
|---|---|---|---|
| Mode | Frequency $\omega_0$ | Exponent $n$ | Diameter coefficient $C$ |
| RBM | 0 | 1 | 248 [a] |
| $D$ | $\omega_D^0$ | 0 | $-16.5$ [b] |
| $G^+$ | 1591 | ... | 0 |
| $G^-$ | 1591 | 2 | $(-45.7,-79.5)$ [c] |
| $M^+$ | $\omega_{M^+}^0$ | 1 | $-18.0$ |
| $M^-$ | $\omega_{M^-}^0$ | 1 | $-16.7$ |
| $G'$ | $\omega_{G'}^0$ | 1 | $-35.4$ |

[a]Reference 5.

[b]This value was obtained using the $E_{\text{laser}}=2.41$ eV. By using the data obtained with $E_{\text{laser}}=1.58$ eV a $-18.9$ value was obtained.

[c]The coefficient *C* for the $G^-$ component is, respectively, $-45.7$ and $-79.5$ $\text{cm}^{-1}$ $\text{nm}^2$ for semiconducting and metallic SWNTs and 1.58, 2.41, and 2.54 eV laser lines were used to obtain the *G*-band experimental results used in the fitting procedure (Ref. 22.)

In Table I are summarized the experimentally determined coefficients for the diameter dependence of several phonon modes observed in SWNT Raman spectra. Both the RBM and *G* band exhibit mode frequencies that do not depend on nanotube chirality but rather have frequencies that are related to the nanotube diameter. The RBM frequency obeys the relation of Eq. (2) and the proportionality coefficient *C* is positive (248 $\text{cm}^{-1}$nm) for isolated SWNTs sitting on a $Si/SiO_2$ substrate, which is very different from the usually negative *C* for the other Raman features. The $\omega_{G+}$ frequency is essentially diameter independent with $\omega_{G^+}=1591$ $\text{cm}^{-1}$, and an analysis considering only the two most intense modes revealed that the lower frequency component $\omega_{G^-}$ shows a diameter dependence of $C/d_t^2$ with a coefficient *C* that depends on whether the SWNT is semiconducting or metallic. The constant *C* for metallic SWNTs (79.5 $\text{cm}^{-1}$ $\text{nm}^2$) is about twice that for semiconducting tubes (45.7 $\text{cm}^{-1}$ $\text{nm}^2$).[22] The results provided here for $\omega_{G^-}$ are obtained by fitting the frequency of the maximum intensity of the $G^-$ feature.[22] This feature can actually be decomposed into up to three peaks with different symmetries,[1,22] but their detailed analysis (involving polarization studies) is not within the scope of this work.

The physics behind the diameter dependence for the lower *G*-band component is still an open issue,[22] and models for the phonon dispersion relations based on both spring constants[24] and *ab initio*[33] calculations predict a weaker $1/d_t$ dependence than that observed experimentally.[22] Very recently, Dubay *et al.*[25] reported, by using highly accurate *ab*

*initio* calculations, that the $G^-$ mode in metallic tubes is significantly softer than in semiconducting tubes due to a Peierls-like mechanism, where a special electron-phonon coupling induces the opening of a gap at the $K$ point. This model is qualitatively in agreement with the experimental results by Jorio *et al.*[22] but the precise diameter dependence is still not well explained.

The $D$, $G'$, and $M$ modes, whose origin relies on the double-resonance process, exhibit a quite different behavior from the RBM and $G$-band modes. First, the modes associated with the double-resonance process are dispersive with regard to the laser excitation energy and exhibit a strong chirality dependence. Since the double-resonance conditions in SWNTs are restricted by the 1D structure for both phonons and electrons, the diameter dependence emerges as a clear picture only when appropriate averages over the chiral angle are made. After performing such averages, the chirality-dependent double resonance effects are effectively averaged out, and we then can evaluate the spring constant effects that are expected to have a $C/d_t$ dependence with $C<0$; i.e., the frequency decreases as the diameter decreases. This is indeed observed for the $D$ band, the $G'$ band, and the combination $M$-band modes, each having slopes of 16.5, 35.4, and 17 $\mathrm{cm}^{-1}$nm, respectively. The very different diameter dependences of the RBM and $G$-band modes provide strong evidence that a different mechanism dominates the Raman scattering for these modes. The $C$ value for the RBM is high compared with modes, such as the $D$-, $G'$-, and $M$-band modes, whose origin comes from the double-resonance process.

### B. $D$ band vs $G'$ band: Diameter dependence and double-resonance effect

In this section we describe the $G'$ band properties and their relation to those of the $D$ band. The same approach that was applied to the $D$ band in Sec. III A is now applied to the second-order $G'$ band, which appears at a frequency of approximately $2\omega_D$. The fit to the experimental data (measured with $E_{\mathrm{laser}}=2.41$ eV) leads to

$$\overline{\omega}_{G'}=2708.1-35.4/\overline{d}_t \tag{3}$$

in analogy to the $D$ band for SWNTs [Eq. (1)]. Both the frequency intercept at $1/\overline{d}_t\rightarrow 0$ and the slope for the $G'$-band data are consistent with the corresponding $D$-band behavior, based on the approximate relation $\omega_{G'}\simeq 2\omega_D$. Furthermore, the $G'$-band frequency of 2D graphite is 2710 $\mathrm{cm}^{-1}$ (taken from Ref. 17) which is close to 2708.1 $\mathrm{cm}^{-1}$, and the slope of 35.4 $\mathrm{cm}^{-1}$nm in Eq. (3) is very close to twice the $D$-band slope of 16.5 $\mathrm{cm}^{-1}$nm in Eq. (1). In principle, we also could do the same $G'$-band analysis for the isolated nanotubes probed with $E_{\mathrm{laser}}=1.58$ eV but a very strong luminescence from the Si substrate in the $G'$-band region does not allow one to get reliable data on this topic.

The experimental observation in 2D graphite that the $G'$-band frequency $\omega_{G'}$ does not exactly satisfy the relation $\omega_{G'}=2\omega_D$ remained an open issue for a long time. Recently, Cançado *et al.*[28] successfully employed double resonance theory to explain the small frequency difference between $\omega_{G'}$ and $2\omega_D$ in detail for 2D graphite. This is associated with the fact that the $D$ band has two peaks (depending on whether the elastic or inelastic scattering event occurs first) and the $G'$ band has two inelastic scattering processes.

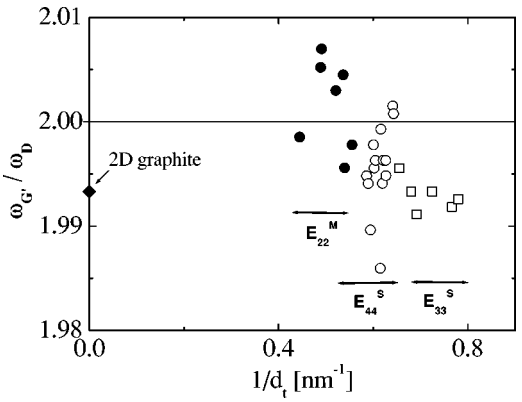


FIG. 3. Plot of the average $\omega_{G'}/\omega_D$ ratio for several isolated SWNTs for which $E_{\mathrm{laser}}=2.41$ eV is resonant with $E_{22}^M$ (solid circles), $E_{33}^S$ (open squares), and $E_{44}^S$ (open circles). The diamond point at $1/d_t=0$ is for 2D graphite (Ref. 28).

In Fig. 3 we show the $\omega_{G'}/\omega_D$ ratio for several isolated SWNTs as a function of $1/d_t$. Similar to other $sp^2$ carbon-based materials, the $G'$-band frequency $\omega_{G'}$ in isolated SWNTs is not exactly centered at 2 times the $D$-band frequency $\omega_D$. However, in contrast to the $D$ band in graphite, the $D$ band in SWNTs is much narrower in linewidth (linewidths down to 7 $\mathrm{cm}^{-1}$ were observed,[34] rather than 65 $\mathrm{cm}^{-1}$ which is observed in 2D graphite[28]). However, the fact that for isolated SWNTs the $G'$-band frequency $\omega_{G'}$ is not twice $\omega_D$ for the $D$ band suggests that the $D$ band similarly originates from two processes (the first scattering event is either by a defect or by a phonon), as in graphite. However, for isolated SWNTs, a spread is observed in $\omega_D$ and $\omega_{G'}$ measured with a single laser line, instead of a single value for $\omega_D$ and $\omega_{G'}$, as occurs for graphite, and this spread in isolated SWNTs seems to be related to the relative position of $E_{\mathrm{laser}}$ with respect to the singularities $E_{ii}$ for each SWNT, which implies different preresonance conditions and that $|E_{\mathrm{laser}}-E_{ii}|$ has some effect on the spectral frequencies.[35]

As can be observed in Fig. 3, the $\omega_{G'}/\omega_D$ ratio at the single-nanotube level seems to exhibit a dependence on $d_t$, but the most important results are that the values of $\omega_{G'}/\omega_D$ are spread out, changing from one tube to another tube, in contrast to the situation in 2D graphite, where $\omega_{G'}/\omega_D$ has a specific value of 1.993.[28] Furthermore, the observed spread, which is due to the trigonal warping effect, thus arises from the different $k_{ii}$ values depending on the $(n,m)$ or $d_t$ of each tube, which is excited by a given laser energy $E_{\mathrm{laser}}$. As a consequence of the detailed difference in the double resonance requirements that depend on the 1D structure of the nanotube, each $(n,m)$ nanotube exhibits different $D$- and $G'$-band properties. From Fig. 3, one can observe that the average $\omega_{G'}/\omega_D$ values for $E_{33}^S$ (1.992) and $E_{44}^S$ (1.998) obtained from Fig. 3 are very close to the value of 1.993 for 2D graphite. It is surprising that the average for metallic tubes

$\omega_{G'}/\omega_D = 2.003$ is so close to 2 and is greater than $\omega_{G'}/\omega_D$ for the semiconducting tubes. The spread of $\omega_{G'}/\omega_D$ from the average for all the $E_{ii}$ subbands is $\sim 0.01$. At present we have no explanation for the apparently different behavior between semiconducting and metallic tubes regarding $\omega_{G'}/\omega_D$. The ratio $\omega_{G'}/\omega_D$ should also depend on the different resonant conditions for the $D$ and $G'$ bands. To get further insights into this effect, an experiment with a tunable laser is needed. This challenging experiment is currently under way.

## IV. SUMMARY

In summary, we have established the diameter dependence of the most important phonons observed in the Raman spectra of isolated single-wall carbon nanotubes. Emphasis was given to the dispersive $D$ and $G'$ modes where we have shown contrasting roles for the quantized electronic states (double-resonance effect) and for the spring constant on affecting the mode frequencies $\omega_D$ and $\omega_{G'}$. The role of the quantized states is dominant for SWNTs when analyzing data within the same van Hove singularity $E_{ii}$, where $\omega_D = \omega_D^{0,i} + C_i/d_t$ (and $C_i > 0$, while $\omega_D^{0,i}$ depends on which electronic subband is in resonance) (Ref. 15) follows the functional dependence on the tube diameter that arises from $k_{ii}(d_t)$ within a small $d_t$ range. The spring constant effect is clarified when we plot the $\omega_D$ and $\omega_{G'}$ data over a large-diameter range, i.e., covering different singularities $E_{ii}$, and over this broad range of tube diameters, we found that $\overline{\omega_D} = \omega_D^0 + C/\overline{d_t}$ (where $C < 0$ and $\omega_D^0$ is the $D$-band frequency for 2D graphite) (see Table I). The spring constant effect, i.e., a decreasing $1/d_t$ dependence, was experimentally found to be the same, within experimental error, for both metallic and semiconducting nanotubes. Furthermore, the $d_t$ dependence for the modes originating from the double-resonance process is different from the non-double resonance modes, such as the $G$ band and the RBM feature. The $\omega_{G'}/\omega_D$ ratio is not exactly 2—nor is it exactly the same as in 2D graphite—but instead of a single value for a given laser energy, the ratio $\omega_{G'}/\omega_D$ varies from tube to tube due to the trigonal warping effect which modifies the double-resonance condition. The average $\omega_{G'}/\omega_D$ ratio for semiconducting tubes is very close to that for graphite, but for metallic tubes the ratio appears to be close to 2. We do not have an explanation for these observations on the $\omega_{G'}/\omega_D$ ratio and further study of these phenomena are underway. Finally, a correlation between the spectral data for isolated SWNTs and for SWNT bundles was successfully made by performing appropriate averages of the results obtained from single nanotube spectra.

## ACKNOWLEDGMENTS

The authors gratefully acknowledge the Professor J.H. Hafner and Professor C.M. Lieber who provided the samples used to carry out the single-nanotube spectroscopy measurements and Professor J. Mendes Filho for useful discussions. The authors A.G.S.F. and A.J. acknowledge financial support from the Brazilian agencies CAPES (PRODOC grant) and CNPq (PROFIX grant), respectively. Part of the experimental work was performed at Boston University at the Photonics Center, operated in conjunction with the Boston University Department of Physics and the Department of Electrical and Computer Engineering. This work also made use of the MRSEC Shared Facilities at MIT, supported by the National Science Foundation under Grant DMR-9400334 and NSF Laser facility Grant No. 97-08265-CHE. The MIT authors acknowledge support under NSF Grant No. DMR 01-16042. R.S. acknowledges a Grant-in-Aid (No. 13440091.) from the Ministry of Education, Japan. We gratefully acknowledge the NSF/CNPq joint collaboration program (NSF Grant No. INT. 00-00408 and CNPq Grant No. 910120/99-4).

*Corresponding author. Electronic address: agsf@fisica.ufc.br

[1] R. Saito, G. Dresselhaus, and M. S. Dresselhaus, *Physical Properties of Carbon Nanotubes* (Imperial College Press, London, 1998).

[2] For an updated review, see M. S. Dresselhaus, G. Dresselhaus, and Ph. Avouris, *Carbon Nanotubes: Synthesis, Structure, Properties and Applications* Vol. 80 of *Springer Series in Topics in Applied Physics* (Springer-Verlag, Berlin, 2001).

[3] M. S. Dresselhaus and P. C. Eklund, Adv. Phys. **40**, 705 (2000).

[4] A. M. Rao, E. Richter, S. Bandow, B. Chase, P. C. Eklund, K. A. Williams, S. Fang, K. R. Subbaswamy, M. Menon, A. Thes, R. E. Smalley, G. Dresselhaus, and M. S. Dresselhaus, Science **275**, 187 (1997).

[5] A. Jorio, R. Saito, J. H. Hafner, C. M. Lieber, M. Hunter, T. McClure, G. Dresselhaus, and M. S. Dresselhaus, Phys. Rev. Lett. **86**, 1118 (2001).

[6] The joint density of electronic states (JDOS) is given by $\mathrm{JDOS}(\hbar\omega) = (1/4\pi^3)\int \delta[E_i^c(k) - E_i^v(k) - \hbar\omega]dk$, where $E_i^c$ and $E_i^v$ are the energies for the $i$th electronic state in the conduction ($c$) and valence ($v$) bands, respectively.

[7] M. S. Dresselhaus, G. Dresselhaus, A. Jorio, A. G. Souza Filho, and R. Saito, Carbon **40**, 2043 (2001), and references therein.

[8] C. Thomsen and S. Reich, Phys. Rev. Lett. **85**, 5214 (2000).

[9] R. Saito, A. Jorio, A. G. Souza Filho, G. Dresselhaus, M. S. Dresselhaus, and M. A. Pimenta, Phys. Rev. Lett. **88**, 027401 (2001).

[10] J. Kürti, V. Zólyomi, A. Grüneis, and H. Kuzmany, Phys. Rev. B **65**, 165433 (2002).

[11] O. Lourie and H. D. Wagner, J. Mater. Res. **13**, 2418 (1998).

[12] C. A. Cooper and R. J. Young, J. Raman Spectrosc. **30**, 929 (1999).

[13] P. M. Ajayan, L. S. Schadler, C. Giannaris, and A. Rubio, Adv. Mater. **12**, 750 (2000).

[14] M. A. Pimenta, A. Jorio, S. D. M. Brown, A. G. Souza Filho, G. Dresselhaus, J. H. Hafner, C. M. Lieber, R. Saito, and M. S. Dresselhaus, Phys. Rev. B **64**, 041401 (2001).

[15] A. G. Souza Filho, A. Jorio, G. Dresselhaus, M. S. Dresselhaus, R. Saito, A. K. Swan, M. S. Ünlü, B. B. Goldberg, J. H. Hafner, C. M. Lieber, and M. A. Pimenta, Phys. Rev. B **65**, 035404 (2002).

[16] J. H. Hafner, C. L. Cheung, T. H. Oosterkamp, and C. M. Lieber, J. Phys. Chem. B **105**, 743 (2001).

[17] H. Wilhelm, M. Lelausian, E. McRae, and B. Humbert, J. Appl. Phys. **84**, 6552 (1998).
[18] R. Saito, G. Dresselhaus, and M. S. Dresselhaus, Phys. Rev. B **61**, 2981 (2000).
[19] M. A. Pimenta, E. B. Hanlon, A. Marucci, P. Corio, S. D. M. Brown, S. A. Empedocles, M. G. Bawendi, G. Dresselhaus, and M. S. Dresselhaus, Braz. J. Phys. **30**, 426 (2000).
[20] S. D. M. Brown, A. Jorio, M. S. Dresselhaus, and G. Dresselhaus, Phys. Rev. B **64**, 073403 (2001).
[21] P. H. Tan, Y. Tang, Y. M. Deng, F. Li, Y. L. Wei, and H. M. Cheng, Appl. Phys. Lett. **75**, 1524 (1999).
[22] A. Jorio, A. G. Souza Filho, G. Dresselhaus, M. S. Dresselhaus, A. K. Swan, M. S. Ünlü, B. Goldberg, M. A. Pimenta, J. H. Hafner, C. M. Lieber, and R. Saito, Phys. Rev. B **65**, 155412 (2002).
[23] A. Grüneis, R. Saito, T. Kimura, L. G. Cançado, M. A. Pimenta, A. Jorio, A. G. Souza Filho, G. Dresselhaus, and M. S. Dresselhaus, Phys. Rev. B **65**, 155405 (2002).
[24] R. Saito, A. Jorio, J. H. Hafner, C. M. Lieber, M. Hunter, T. McClure, G. Dresselhaus, and M. S. Dresselhaus, Phys. Rev. B **64**, 085312 (2001).
[25] O. Dubay, G. Kresse, and H. Kuzmany, Phys. Rev. Lett. **88**, 235506 (2002).
[26] S. D. M. Brown, A. Jorio, P. Corio, M. S. Dresselhaus, G. Dresselhaus, R. Saito, and K. Kneipp, Phys. Rev. B **63**, 155414 (2001).
[27] M. J. Matthews, M. A. Pimenta, G. Dresselhaus, M. S. Dresselhaus, and M. Endo, Phys. Rev. B **59**, R6585 (1999).
[28] L. G. Cançado, M. A. Pimenta, R. Saito, A. Jorio, L. O. Ladeira, A. Grüneis, A. G. Souza Filho, G. Dresselhaus, and M. S. Dresselhaus, Phys. Rev. B **66**, 035415 (2002).
[29] C. A. Cooper, R. J. Young, and M. Halsall, Composites, Part A **32**, 401 (2001).
[30] U. D. Venkateswaran, A. M. Rao, E. Richter, M. Menon, A. Rinzler, R. E. Smalley, and P. C. Eklund, Phys. Rev. B **59**, 10 928 (1999).
[31] A. M. Rao, J. Chen, E. Richter, U. Schlecht, P. C. Eklund, R. C. Haddon, U. D. Venkatesvaran, Y. K. Kwon, and D. Tománek, Phys. Rev. Lett. **86**, 3895 (2001).
[32] V. W. Brar, Ge. G. Samsonidze, M. S. Dresselhaus, G. Dresselhaus, R. Saito, A. K. Swan, M. S. Ünlü, B. B. Goldberg, A. G. Souza Filho, and A. Jorio, Phys. Rev. B **66**, 155418 (2002).
[33] J. Maultzsch, S. Reich, C. Thomsen, E. Dobardzic, I. Milosevic, and M. Damnjanovic, Solid State Commun. **121**, 471 (2002).
[34] A. Jorio, A. G. Souza Filho, V. W. Brar, A. K. Swan, M. S. Ünlü, B. Goldberg, R. Saito, J. H. Hafner, C. M. Lieber, G. Dresselhaus, and M. S. Dresselhaus, Phys. Rev. B **65**, 121402(R) (2002).
[35] A. G. Souza Filho, A. Jorio, A. K. Swan, M. S. Ünlü, B. B. Goldberg, R. Saito, J. H. Hafner, C. M. Lieber, M. A. Pimenta, G. Dresselhaus, and M. S. Dresselhaus, Phys. Rev. B **65**, 085417 (2002).